Continuous ESD Monitoring System for Manufacturing

Patrick Xu (1), Kwanghoi Koo (1), Oscar Tang (2), Noah Tatman (1)

(1) Amazon, 1100 Enterprise Way, Sunnyvale, CA 94089 USA, tel.: 650-426-1100,
e-mail: patxu@amazon.com, kwanghoi@lab126.com, and ntatman@amazon.com

(2) Amazon, 25F, Building B, Shenzhen International Innovation Center, Shenzhen, Guangdong, P.R. China,
tel.: 0755-3327-8002, email oscart@amazon.com

Abstract - Electro-Static Discharge (ESD) damage is a common failure mode in the manufacturing process. This paper introduces a continuous ESD monitoring system for New Product Introduction (NPI) line ESD qualification and early detection of potential static charges buildup on devices to defuse the ESD damage risk.

I. Introduction

Debugging ESD failures, especially low failure rate damage, is extremely difficult; it is sometimes almost impossible to reproduce failures and determine the process responsible. Even with regular ESD audits based on industry standards (ANSI/ESD S20.20) and additional in-line ESD checks, eliminating the risk of ESD failure is difficult. Furthermore, changes related to manufacturing processes, material configurations, or production run rates in product builds can increase risk for ESD management.

This paper presents a continuous ESD monitoring system to rapidly and accurately identify and localize static charge buildup on ESD sensitive components. Current audit methods only provide a momentary snapshot of the ESD management process and the status of an assembly line, whereas continuous monitoring provides a comprehensive static field history of each PCBA on a line. The system generates static charge heat maps, which highlight occurrences and locations of charge buildup, greatly reducing the difficulty of ESD risk assessment and debugging. The accumulated data can also make decisions regarding the build readiness of a line when unexpected ESD failures occur and assess the efficacy of preventative measures. Preliminary line data demonstrate that the fixture measurements correlate with line station data with ionizers or without ionizers installed and could be used to determine where to install ionizers.

For continuous ESD monitoring, there are examples of industry ESD voltage monitoring using a contact electrometer [1] or electrostatic discharge measurement with an antenna to detect discharge events [2-3]. However, these methods are either expensive or complicated to install which limits their usage in real production lines. The system the authors have developed utilized noncontact fieldmeters to monitor the E-field. The advantages of the low-cost and agile setup of the monitoring system allow for wider deployment between numerous stations on the assembly line.

II. Continuous ESD Monitoring System Architecture

ESD fieldmeters are placed at the pre-defined locations in the manufacturing line to collect the E-field data from interested ESD susceptible (ESDS) items. The analog data from the fieldmeter are converted to digital data by analog to digital converter (ADC) and uploaded to a local server through an Ethernet interface as shown in Figure 1.

To allow the fixture to be placed en masse on the line, the fixture boasts a low bill of material (BOM) cost and primarily utilizes off-the-shelf components to aid in ease in installation and deployment. The fixture can be readily mounted on SMT line environments using off-the-shelf methods such as C-clamps or L brackets.

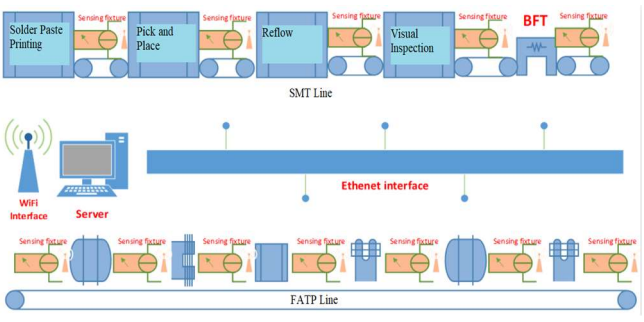

Figure 1. Example of fixture deployment plan

The ESD monitoring system is a motor-driven mechanical fixture comprised of three main blocks: a motor-driven fixture, a power hub, and a control & sensor suite as shown in Figure 2. The actual fixture design is shown in Figure 3.

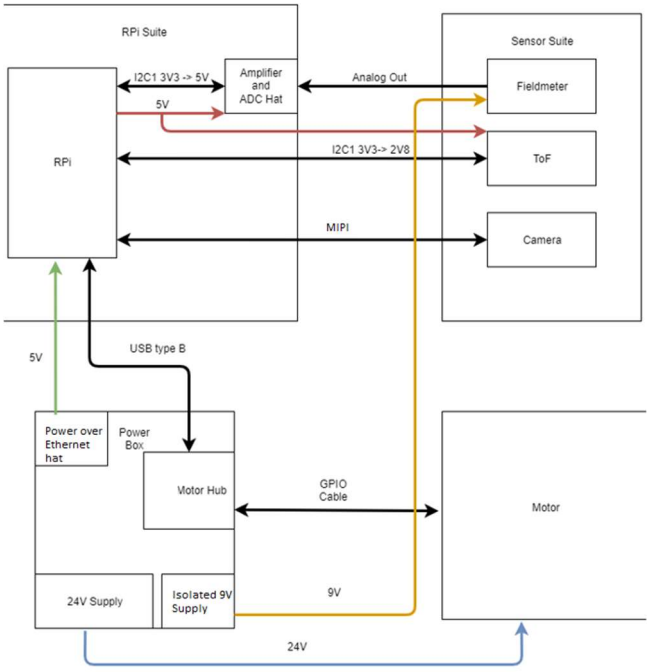

Figure 2. Continuous ESD monitoring system block diagram

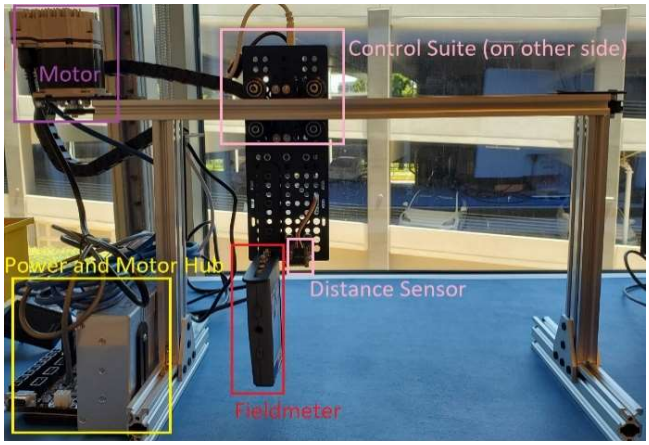

Figure 3. SMT fixture design

The fixture is a mechanical fixture that will scan PCBs or devices on the surface mount technology (SMT) or final assembly, test and packing (FATP) line. The fixture is mounted at a fixed location, and will sweep above the device under test (DUT) as it travels under the fixture. The current fixture design is specific to SMT line monitoring and only features one axis of motion along the width of the SMT line.

The power hub includes the main power supply for the system along with an emergency stop switch. It also includes a motor control hub to allow for software-API based motor control and telemetry readout.

The control & sensor suite houses the control electronics and various sensors utilized by the fixture. It includes an ESD fieldmeter, distance sensor, and camera (not enabled on the current fixture). It also includes a signal conditioning circuit for the fieldmeter output to isolate and amplify the output for improved resolution and denoising. The fieldmeter ground reference has an equipotential bonding to the mechanical ground to provide the fieldmeter measurement ground reference. The control and sensor electronics are mounted on the fixture gantry in the current design, and are swept across the width of the SMT line to scan the DUT.

The fixture captures a 3D E-field heat map for all DUT measured by the fixture. These logs allow for the detection and position estimation of charge buildup events on the line. One example E-field heat map is shown in Figure 4.

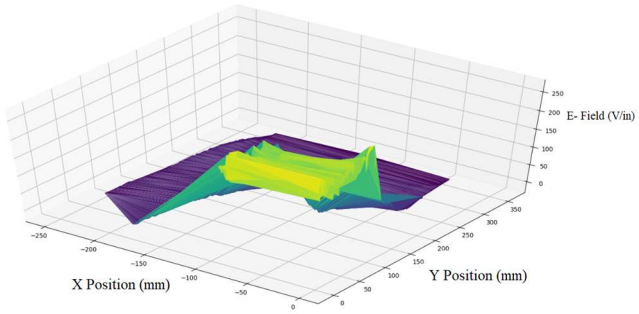

Figure 4. E-field heat map of a test surface with a 240 V static voltage region in the bottom right corner

III. Continuous ESD Monitoring System Calibration

A. Overview of Calibration Process

The sensor and fixture performance were validated over multiple trials using fixed voltage calibration boards and PCBs. The current calibration board utilizes a boost converter to generate an adjustable high voltage static output. This output is fed to a large copper plane that is then placed underneath the fieldmeter to provide a reference calibration voltage. The calibration board can also be arranged such that the board itself contains multiple output zones, such as alternating between GND and high voltage output. This can be utilized to characterize the fixture performance while the fixture is in motion, as the handheld fieldmeter accuracy will

decrease if it is measured while in motion compared to remaining stationary.

The current calibration process is meant to provide a software method to zero the fieldmeter with a series of stationary measurements. This allows the user to calibrate the meter without having to physically zero the sensor prior to use or in-between measurements. This assumes a static DC offset across the full measurement range. There are two primary reasons for this assumption: (1) The calibration is meant to provide automated SW-based method of zeroing the fieldmeter instead of having to press the "Zero" button on the fieldmeter itself. The zeroing process on the meter itself applies a DC offset for calibration; (2) Prior data has demonstrated that the offset is static, accounting for minor fluctuation due to measurement noise/error or slight fluctuations in the reference source.

The calibration process is currently performed when initializing the fixture each time. However, since the calibration process itself may include several potential sources of error, e.g. measurement noise, and variation in the output voltage, the current calibration process utilizes a series of reference voltage calibrations compared to a singular measurement.

The general fixed position calibration process is as follows:

1. The system expects up to three pre-set reference voltages. For each voltage:
   a. The operator positions the calibration board set to the reference voltage underneath the fieldmeter.
   b. The system captures 100 voltage and distance samples over one second.
   c. The system averages the measurement distance and voltage and scales the average voltage according to the measurement distance using the following equation:

$$V_{scaled} = V_{meas} * (\frac{D_{meas}}{1\ inch})$$

   d. The system calculates the average offset of the measurement.
2. After the averages have been calculated, the system generates a linear regression based on the measured offsets and scaled voltages to calculate the intercept (a) and slope (b):

$$V_{offset} = a + b * V_{scaled}$$

$$V_{out} = V_{scaled} - V_{offset}$$

However, the current distance sensor is too inaccurate to provide accurate distance scaling, so the current system only utilizes the reference distance measurements to ensure that the fieldmeter is mounted at one inch, but is not used in scaling the measurement voltage. It was observed that the added measurement noise and precision limitations of the existing distance sensor affected the voltage output accuracy.

If the offset is static, the slope of the linear regression will be very small or near zero. During data collection, the slope is utilized to confirm that the system setup matches expectations. The current calibration process utilizes 0 V, 240 V, and 0 V measurement for the reference voltage levels (Figure 5 & 6).

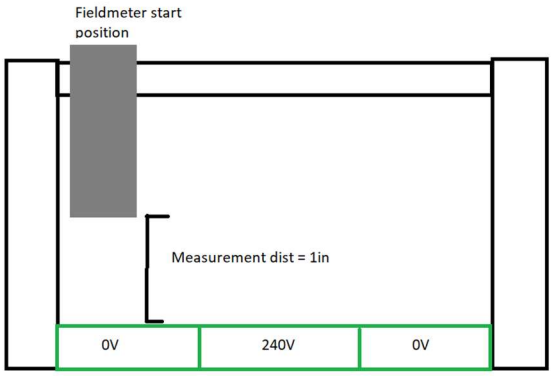

Figure 5. Calibration measurement setup showing three voltage zones

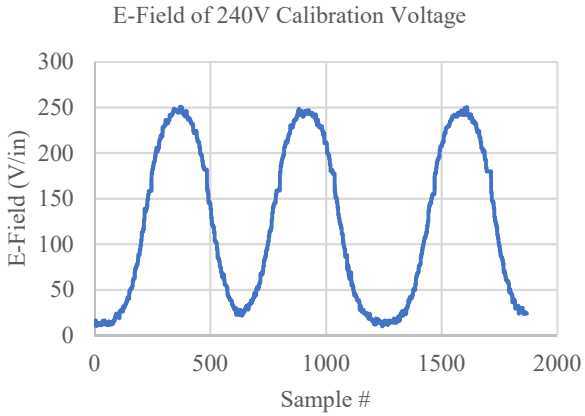

Figure 6. E-field data vs time on calibration board with three voltage zones (0 V, 240 V, 0 V)

B. Characterization of Fixture Performance

The fieldmeter performance is affected by two primary factors: the measurement distance and the measurement speed.

The fieldmeter has an optimal measurement range at one inch and has +/-10% accuracy from -2 kV to +2 kV at this distance. The measured voltage must be scaled accordingly with the distance of the fieldmeter to the

DUT. The output voltage scales linearly with respect to the measurement distance, e.g. the fieldmeter report 1 kV at 1 inch, 2 kV at 0.5 inch, and 500 V at 2 inches when measuring a 1 kV charge. The current fixture design fixes the fieldmeter at one inch to minimize potential sources of error, such as measurement accuracy of the fixture's distance sensor.

The current fieldmeter reports a sample rate of 25 Hz. Thus, there is a time lag between the fieldmeter crossing a charge region and updating its analog output. Furthermore, there are limitations regarding the resolution of the voltage measurement, as the fieldmeter may fail to accurately detect a charge region if it passes over the area too quickly. Thus, the sample rate is a limiting factor in configuring the maximum fixture sweep speed and line speed.

This lag was observed and characterized by measuring a localized 1 kV impulse located in the center of the fixture travel distance (Figure 7). The fixture was run at several speeds to observe how the offset with the fixture speed. The impulse was generated with a handheld static field generator, with a 2.35 mm diameter cylindrical antenna. The meter antenna was placed parallel to the measurement surface.

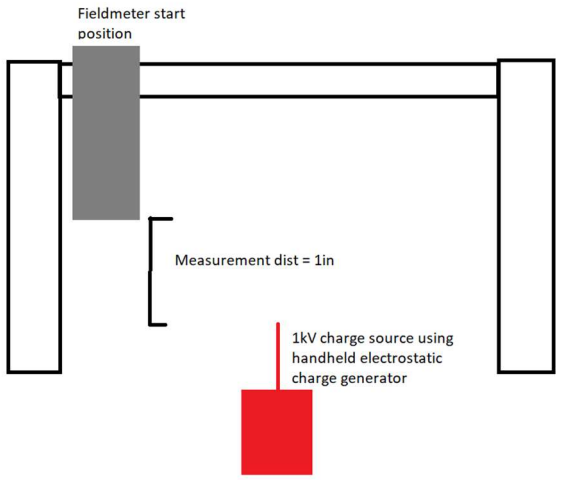

Figure 7. Impulse test measurement setup with 1 kV localized charge source

Given that the DUT was a highly localized charge source, the ideal heat map would show a unimodal distribution. However, except for very low speed measurements (Figure 8), the fixture data showed a bimodal distribution (Figure 9 & 10). The gap between these bimodal peaks was exacerbated at higher speeds. It was observed that there was an offset of the analog output in both fixture travel directions corresponding to ~30-50 ms. The measurement lag resulted in a shift of the measurement peak in both directions, thus resulting in a skewed bimodal measurement pattern. The gap widens at higher speeds as the time gap is relatively consistent across speeds.

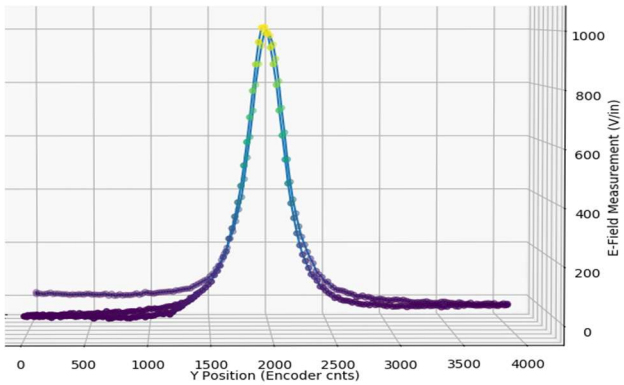

Figure 8. Y-Z view of E-field heat map for a measurement of a localized 1kV impulse at 3% (30 mm/s) max fixture speed

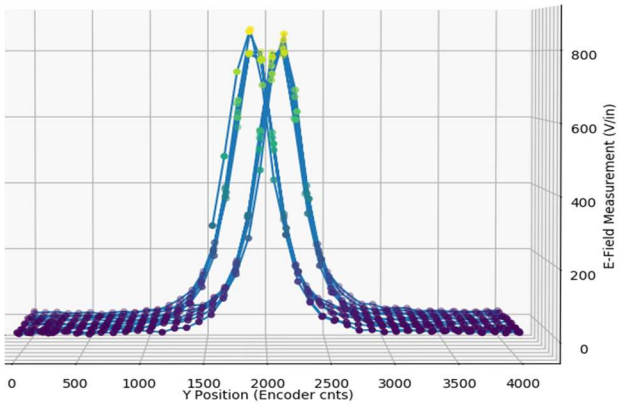

Figure 9. Y-Z view of E-field heat map for a measurement of a localized 1kV impulse at 12% (120 mm/s) max fixture speed

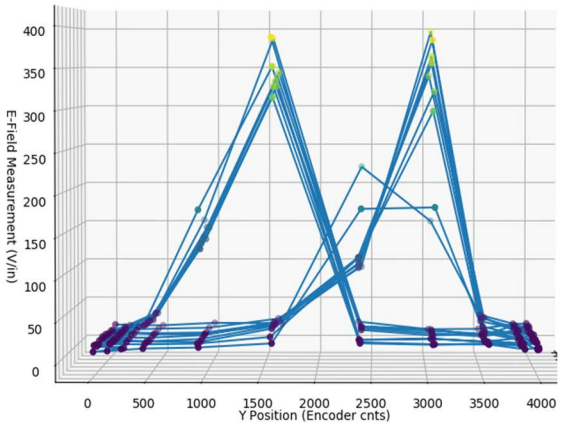

Figure 10. Y-Z view of E-field heat map for a measurement of a localized 1kV impulse at 100% (1 m/s) max fixture speed

Figure 11 illustrates the observed time gap between the fixture travelling over the impulse position (2000 encoder counts) compared to where the peak was

recorded in the datalog at various speeds. This provides an estimation of the time gap. There are several factors, such as when the fieldmeter output refreshed with respect to the impulse, that affected the accuracy of this measurement, but the figure provides a reference of the time lag.

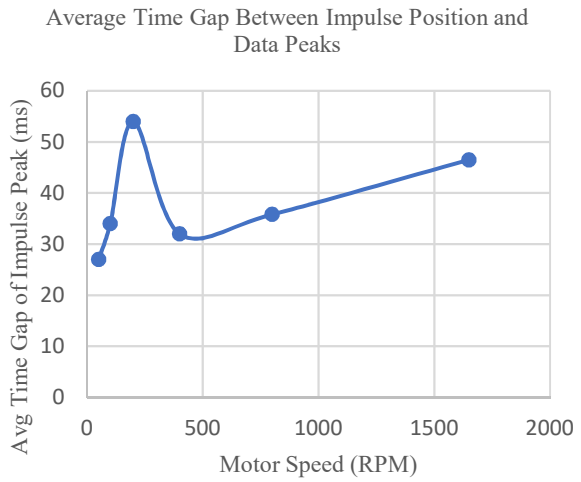

Figure 11. Measured time lag observed between the impulse position and heat map peaks vs motor speed

In addition to the time lag in the measurement, the output also becomes attenuated at higher speeds, shown in Figure 12. Notably, the peak voltage at 100% speed was only 400 V compared to the expected 1 kV. This is due to the sample rate of the meter itself. The high speed and small measurement area results in the meter's sensor not fully coupling to the DUT E-field, resulting in reduced measurement output.

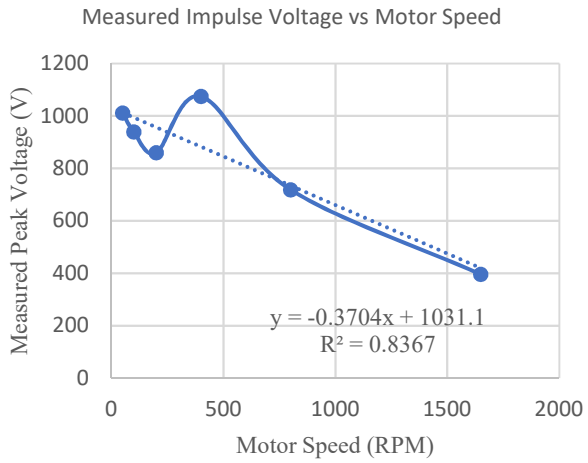

Figure 12. Measured peak impulse voltage measured vs motor speed

These limitations indicate that the current fieldmeter is not capable of high-speed position mapping of voltage. However, at lower speeds, the fieldmeter is still able to capture charge buildup on the DUT, so while the E-field position mapping is not highly accurate at higher speed, it can still be utilized to inform the operator of overall charge buildup on the DUT.

However, while the fixture exhibits a position skew and attenuated voltage at high speeds, the fixture measurement results are highly consistent. Voltage data indicates voltage buildup position and magnitude exhibit high precision over multiple bidirectional sweeps of a stationary DUT. The overall range of the measurement peaks is within the +/-10% tolerance of the fieldmeter specification.

Due to these limitations, the current 500 mm travel distance fixture was deployed at 30% max speed (300 mm/s) for the SMT production line study. The current line speed was around 100 mm/s. At the given speed conditions, the voltage peak magnitude and position may be skewed. However, these speeds were selected to balance the voltage accuracy compared against the scanning coverage, so that while the accuracy is compromised, the fixture can perform two to three back-and-forth sweeps of each DUT.

IV. Continuous ESD Monitoring Result from SMT line

A. E-field Heat Map of Individual Panel

Figure 13 shows the E-field contour plot on one panel in a size of 275 mm x 190 mm and the overall size is 340 mm x 250 mm when counting in the metal carrier frame. The panel includes six PCBs (dashed line box) in three rows along with the conveyor moving direction. The black dots represent the actual E-field measurement locations. Around 230 data points of E-field were collected for this panel. The system tracked the Y position (perpendicular to the conveyor moving direction) of the sensor across the DUT and mapped the measured E-field strength to the position.

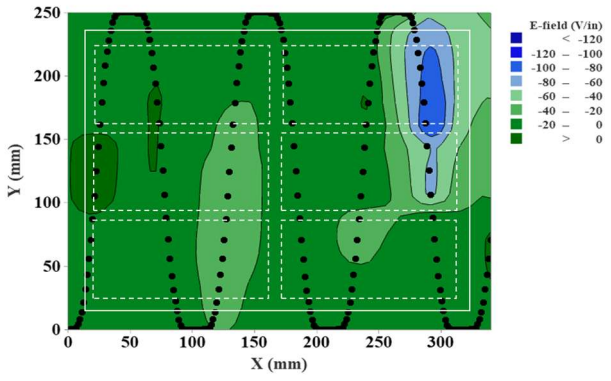

Figure 13. E-field heat map of a panel

B. E-field Plot of Panels in SMT Line

This is one example of ESD continuous monitoring result of one SMT line. A general SMT line includes bare board load, applying solder paste (SP), post solder paste inspection, pick and place (P&P), auto visual inspection (AOI) post P&P, adding the metal shielding can, IR reflow, AOI post reflow, and unload. This process is repeated for the double-sided board. Five locations were selected for the data collection on the component side (CS) of the panel: (1) bare board; (2) post of applying SP; (3) before AOI after P&P; (4) before reflow; (5) after reflow. At each location, the E-field data collection was conducted on around 100 panels with 150 to 250 data points for each panel depending on the conveyor/line speed at different locations. The dotplot graph visualized the E-field distribution at each location as shown in Figure 14.

The manufacturer can define the E-field control limit at the panel level to evaluate the ESD control robustness. It is essential to consider the peak E-field attenuation effect when both fieldmeter and panel are moving during the data collection. A safe factor needs to be considered to define the E-field control limit based on the peak E-field drop percentage vs. moving speed as shown in Figure 12.

When the control limit is defined, it is possible to calculate the process performance index (Ppk) to quantify the ESD management performance at specific location. If the control limit is set to be +/- 150 V/in, the calculated Ppk for the bare board distribution is 1.21 as shown in Figure 15. For the nonnormal distribution, the common practice is to find the best fitted distribution and estimate the Ppk using the fitted line. When the Ppk value is less than 1.33, the deployment of ionizers can be considered to reduce the E-field variance for that process if it is sensitive to ESD damage.

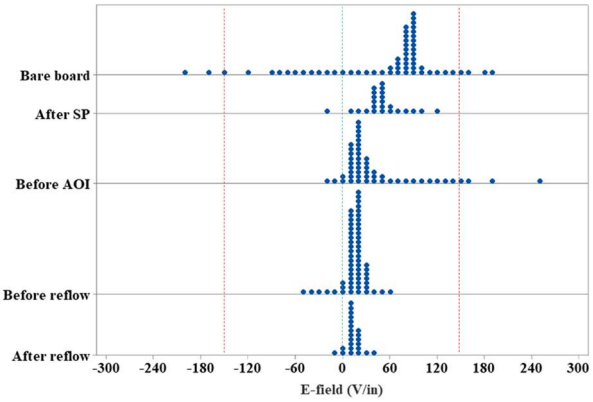

Figure 14. Dotplot of E-field at different SMT locations

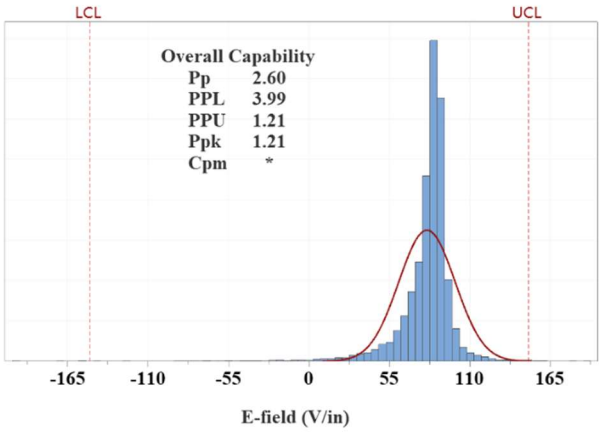

Figure 15. Process capability report for bare board

V. Future Work

A. Data Display from Website

The collected datalogs will be uploaded to the line's local manufacturing data server to track and provide a comprehensive history of all PCBAs and DUTs on the line. The datalogs will be uploaded after each scan in real-time to allow for immediate alerts to excessive charge events and provide analytics. By integrating the datalog collection with the existing line management software, the system will provide a seamless addition for ESD management and tracking functionality.

B. Design Optimizations

There are several planned improvements to the current SMT line fixture design:

1. Improvements to the fieldmeter and sensor design.
   a. There are ongoing investigations into alternate sensor designs and vendors that allow for higher sample rate to improve measurement accuracy at higher speeds.
   b. There are also investigations into sensor array designs, utilizing multiple sensors or fieldmeters arranged in a linear array to capture a larger measurement area, which would allow for reduced fixture speed or travel distance.
2. Improvements to the distance sensor.
   a. There are investigations into alternate low-cost distance sensors, such as alternate time of flight (ToF) or lidar sensors. Improving the sample rate and measurement accuracy will allow for more accurate distance calibration of the measured voltage.

C. FATP Fixture Design

In addition, there are other investigations regarding design adjustments to adapt the current fixture to FATP line stations. There are several notable differences and challenges with this design adjustment.

1. The fixture must include a vertical motor axis for Z axis motion.
2. The DUT's form factor and placement are no longer constant, unlike a PCB panel at SMT. The DUT may be irregular in shape, placed at different locations with respect to the fixture, and may have changes in height over the DUT surface, requiring the fixture to consistently adjust the sensor height to insure measurement accuracy. The sensor itself must also be adjusted quickly enough to not interfere with the DUT itself.
3. The fixture ideally should only scan the DUT surface itself and not scan past the DUT edge. This is to minimize risk of false positives if the fixture detects noise or erroneous measurements if it measures past the DUT. Furthermore, if the fixture sweeps across its full distance instead of only the DUT surface, there is significant time lost during the measurement not actively scanning the device, resulting in large measurement gaps across the DUT surface. The fixture thus must actively track the DUT shape.

The challenges regarding DUT form factor tracking necessitate the use of computer vision (CV) functionality to accurately detect and track the device. There are several notable challenges regarding the use of CV in the fixture design. CV algorithms, particularly machine learning (ML) based models, are computationally expensive. The limited memory and bandwidth of the Raspberry Pi (or another equivalent single board PC) does not allow for the use of ML-based classifiers or models. Thus, the CV functions used must rely on traditional methods of image segmentation, which are less robust under variable DUT, lighting, and test conditions.

The team has investigated several approaches regarding FATP monitoring, but is currently prioritizing the optimization of the SMT fixture.

VI. Conclusion

The continuous ESD monitoring system achieves quantitative E-field data collection and provides insights into assessing ESD management maturity. The system provides opportunity to enhance ESD management robustness beyond the umbrella of conventional ESD audits. The system provides a systematic method of identifying risky processes and optimize ionizer deployment efficacy.

While the current system performance is limited and cannot yet generate accurate position heat maps, it can identify the approximate position and presence of E-field buildup. The low cost and real time data collection features of the system allow for real-time line monitoring to inform the user of ESD events and handling concerns.

VII. Acknowledgments

The authors would like to acknowledge the guidance and help from the Amazon teams and partners. The authors would also like to acknowledge Marcus Koh for providing feedback.

VIII. References

[1] A. Wallash, "Continuous voltage monitoring techniques for improved ESD auditing," 2003 Electrical Overstress/Electrostatic Discharge Symposium, 2003, pp. 1-8.

[2] T. J. Maloney, "The Case for Measurement and Analysis of ESD Fields in Semiconductor Manufacturing," 2018 IEEE Symposium on Electromagnetic Compatibility, Signal Integrity and Power Integrity (EMC, SI & PI), 2018, pp. 396-401.

[3] A. Andersen and J. R. Dennison, "Wireless Antenna Detection of Electrostatic Discharge Events," in IEEE Transactions on Plasma Science, vol. 47, no. 8, pp. 3867-3871, Aug. 2019.